JACS
JOURNAL OF THE AMERICAN CHEMICAL SOCIETY

COMMUNICATION

pubs.acs.org/JACS

Crystalline Covalent Organic Frameworks with Hydrazone Linkages

Fernando J. Uribe-Romo,[†,§] Christian J. Doonan,[†,∥] Hiroyasu Furukawa,[†] Kounosuke Oisaki,[†,⊥] and Omar M. Yaghi*[,†,‡]

[†]Center for Reticular Chemistry, Center for Global Mentoring, Department of Chemistry and Biochemistry, University of California, Los Angeles, 607 Charles E. Young Drive East, Los Angeles, California 90095, United States

[‡]Graduate School of EEWS, Korea Advanced Institute of Science and Technology, Daejeon 305-701, Korea

Supporting Information

ABSTRACT: Condensation of 2,5-diethoxyterephthalohydrazide with 1,3,5-triformylbenzene or 1,3,5-tris(4-formylphenyl)benzene yields two new covalent organic frameworks, COF-42 and COF-43, in which the organic building units are linked through hydrazone bonds to form extended two-dimensional porous frameworks. Both materials are highly crystalline, display excellent chemical and thermal stability, and are permanently porous. These new COFs expand the scope of possibilities for this emerging class of porous materials.

In the chemistry of linking molecular building blocks with strong bonds to make extended structures (reticular chemistry), it is critical, and often a challenge, to find the precise reaction conditions that lead to crystalline materials. This "crystallization problem" has been overcome for the joining of metal ions with organic units using M−O and M−N bonds to make what has become a large class of porous metal−organic frameworks.[1] However, the problem becomes particularly acute in making covalent organic frameworks (COFs),[2] in which the organic units are composed entirely of light atoms and joined by covalent bonds (e.g., C−C, C−N, C−O). In this regard, only recently has success been achieved, and polycrystalline COF materials have been assembled using boronate,[1−12] borosilicate,[13] imine,[12,14] and triazine[15] linkages. The porous COF structures thus prepared have extremely low densities,[3] unusual gas adsorption properties,[16−23] and electronic conductivity.[11,12] In view of the almost limitless number of chemical linkages and the wide range of possible materials that could be achieved through any one kind of linkage, it is important to develop means of making crystalline COF materials with new strong organic linkages. Here we show how two crystalline mesoporous COFs, COF-42 and COF-43, can be made by condensation of easily accessible hydrazine and aldehyde organic building blocks to give hydrazone-linked structures whose crystallinity is controlled by the well-known pH-dependent reversibility of hydrazone linkages.[24,25] We also show that these COFs have permanent porosity with high surface area, adjustable pore size, and exceptional chemical stability.

COF-42 and COF-43 (Scheme 1) were synthesized by the reversible dehydration of 2,5-diethoxyterephthalohydrazide and 1,3,5-triformylbenzene or 1,3,5-tris(4-formylphenyl)benzene in mixtures of mesitylene, 1,4-dioxane, and aqueous acetic acid in flame-sealed tubes.[26] The use of this combination of solvents

Scheme 1. Synthesis of COF-42 and COF-43 by Condensation of Linear 2,5-Diethoxyterephthalohydrazide Building Blocks (Red) with Trigonal-Planar 1,3,5-Triformylbenzene (Blue) or 1,3,5-Tris(4-formylphenyl)benzene (Blue) to Form COF-42 and COF-43 (Cavity Sizes Are Indicated)

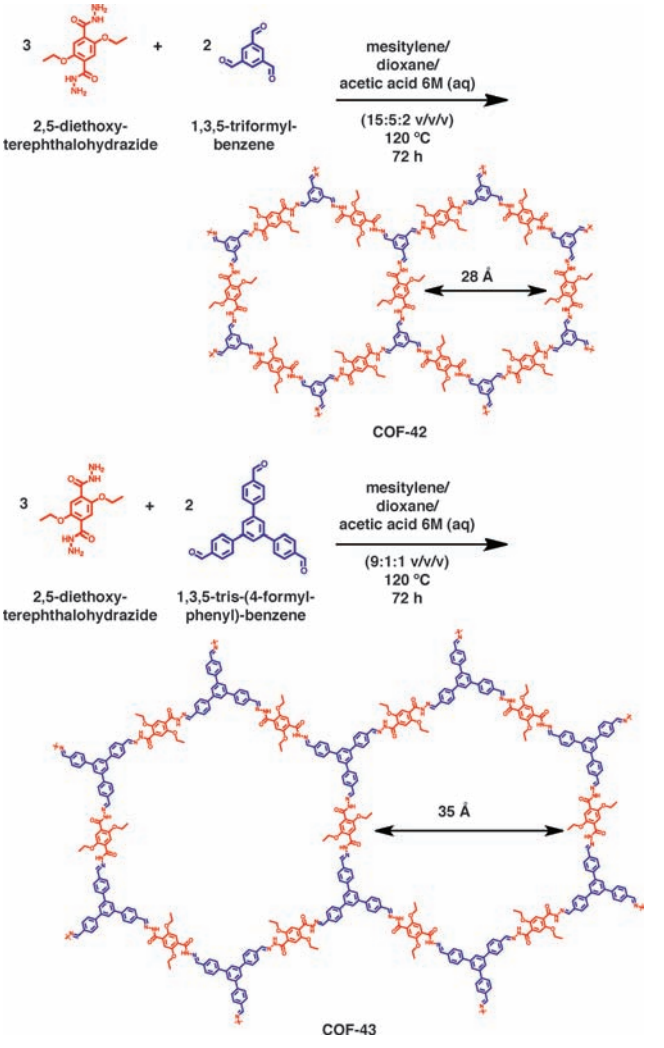

Received: May 23, 2011
Published: July 01, 2011

provided reaction conditions for crystalline samples, and slight variations of the solvents ratios and the amount of acid resulted in materials with very poor or no crystallinity.

Both COF-42 and COF-43 were obtained as pale-yellow microcrystalline powders that remained insoluble in common organic solvents such as alcohols, acetone, chloroform, ethers, acetonitrile, *N*,*N*-dimethylformamide, and dimethyl sulfoxide. The COF materials were immersed in a high-vapor-pressure solvent to remove occluded guests, after which the solvent was removed by heating under dynamic vacuum. Elemental analyses performed on the guest-free samples were in good agreement with the expected chemical formulas of $C_9H_9O_2N_2$ and $C_{15}H_{13}O_2N_2$ for COF-42 and COF-43, respectively.[27]

The molecular connectivity and integrity of the molecular building blocks of guest-free COF-42 and COF-43 were assessed by Fourier transform IR (FT-IR) and ^{13}C cross-polarization with magic-angle spinning (CP-MAS) NMR spectroscopies. Data were collected on the starting materials of both COF materials and the molecular model compound *N*′-benzylidenebenzohydrazide. The FT-IR spectra of COF-42 and COF-43 showed stretching modes at 1621−1605 and 1226−1203 cm^{-1} that are characteristic of $\nu_{C=N}$ moieties.[14] These band assignments were confirmed by the observation of analogous features in the FT-IR spectrum of the molecular model compound. Additional support for the formation of the extended COF network was provided by close analysis of the carbonyl stretching mode of the amide unit. In the COF materials, the $\nu_{C=O}$ band was observed at 1659 cm^{-1} while the corresponding bands in the starting material and the model compound were observed at 1612 and 1643 cm^{-1}, respectively. This shift can be interpreted as a weakening of the $\nu_{C=O}$ bonds as a result of resonance with the imine, as has been observed in molecular hydrazones.[28,29] It is also noteworthy that no signals for the carbonyl $\nu_{C=O}$ stretching modes of the aldehyde groups in the starting materials (1689−1697 cm^{-1}) were observed in the FT-IR spectra of the COFs. ^{13}C CP-MAS NMR analysis provided further confirmation that the molecular backbones of COF-42 and COF-43 are constructed from hydrazone links. The presence of a C═N bond formed by the condensation of the starting materials was established by a characteristic resonance signal at 149 ppm in the spectra of both COFs. Similar resonances were observed in the ^{13}CP-MAS NMR spectra of the carbon of the C═N bond in the model compound (150 ppm) and the carbon atom in COFs constructed from imine links.[14] To assess fully the correspondence of this signal with the imine carbon, we performed a cross-polarization contact time variation experiment, which shows different trends of increasing intensity for carbons with different protonation states.[30] With the exception of the imine, all of the resonance signals between 120 and 160 ppm corresponded to quaternary carbons (aromatic and amide); therefore, we expected the intensity of the imine carbon signal to be significantly different from those of the rest of the signals in the same range (Figure S9 in the Supporting Information).

Powder X-ray diffraction (PXRD) measurements were performed on samples of COF-42 and COF-43 to determine their crystallinity. Figure 1 shows the experimental PXRD patterns of the two COFs, which were indexed on the basis of a primitive hexagonal lattice. The raw data were compared to models of possible crystal structures that can be obtained from linking the trigonal and linear building blocks. Since the hydrazone moiety should be approximately coplanar with the aromatic rings because of resonance effects and internal hydrogen bonding,[31] it

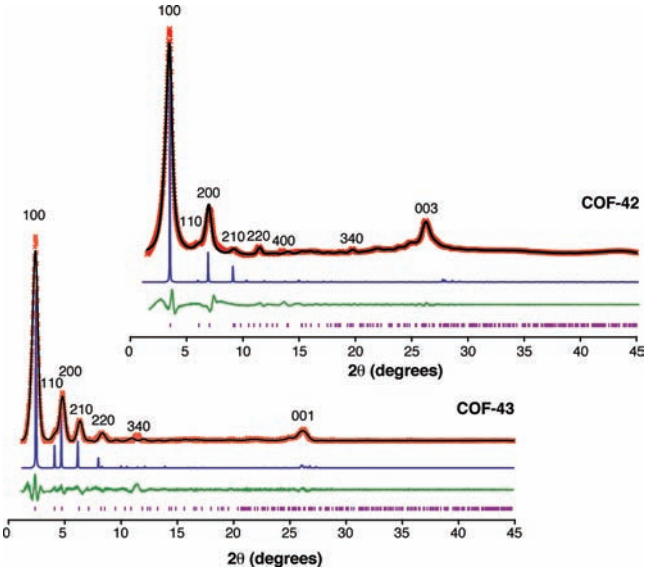

Figure 1. Indexed experimental (red) and refined (black) PXRD patterns of guest-free COF-42 (top) and COF-43 (bottom) after Pawley refinement, compared to the calculated pattern (blue) from the simulated crystal model. The difference plot is indicated in green. Purple ticks indicate the positions of reflections.

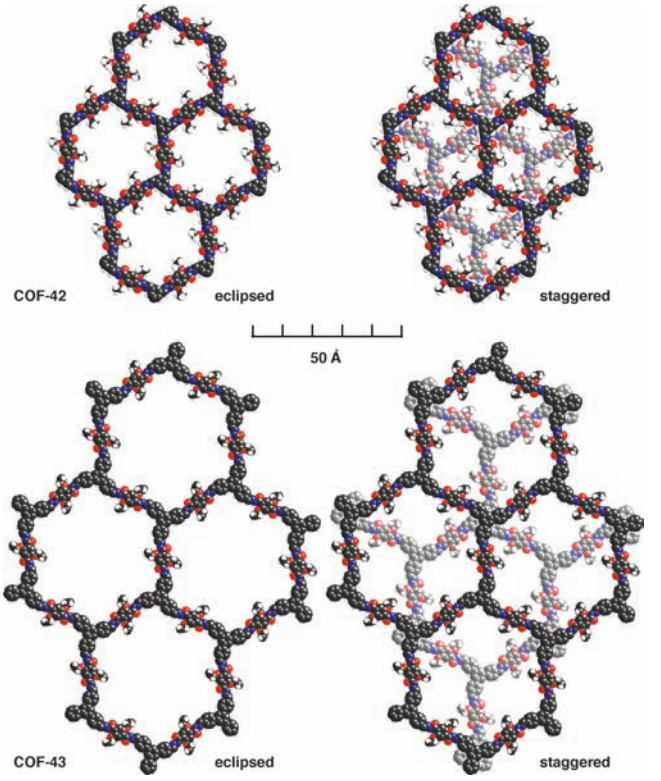

Figure 2. Space-filling models of COF-42 and COF-43 in both extreme packing modes, eclipsed (**bnn** topology) and staggered (**gra** topology). The scale is inset. Atom colors: C, black; H, white; O, red; N, blue.

was anticipated that two-dimensional (2D) trigonal layers (Figure 2) would be formed. These layers can pack in eclipsed **bnn** ($P6/m$) or staggered **gra** ($P6_3/m$) modes.[32] Analysis of the

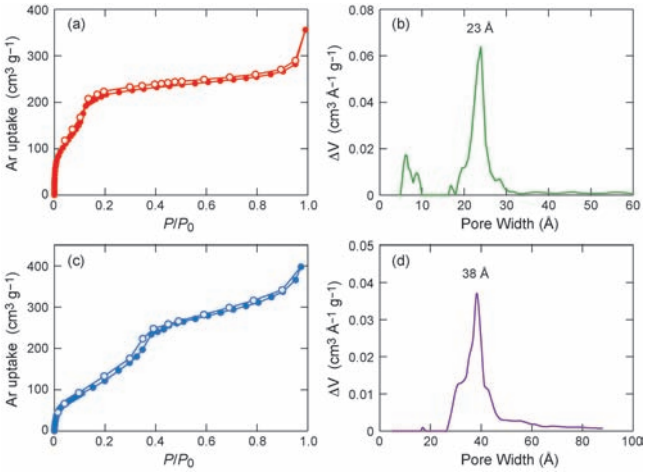

Figure 3. (left) Ar adsorption (●) and desorption (○) isotherms of (a) COF-42 and (c) COF-43. (right) Pore size distributions of (b) COF-42 and (d) COF-43. The average pore sizes are indicated in the corresponding plots.

PXRD pattern of COF-42 indicated peaks with *d* spacings of 25.57, 17.06, 12.81, 9.63, and 6.29 Å, corresponding to the 100, 110, 200, 210, and 220 diffraction peaks in simulations for both **gra** and **bnn** structures, as modeled using *Materials Studio*.[33] In addition, a peak at 3.29 Å correlating with the value of the interlayer distance was observed. The PXRD pattern for COF-42 was then indexed on a primitive hexagonal unit cell and refined using the Pawley method in the Reflex module of *Materials Studio*, yielding cell parameters a = 28.827(15) Å and c = 9.739(12) Å (residuals: R_p = 5.23%, R_{wp} = 6.62%). Notably, the refinement process required that the c cell parameter be 3 times the interlayer distance (c' = 3c for the **bnn** model). This modified value can be attributed to faults within the stacking of the 2D layers[34] and had no significant effect on the proposed models. The PXRD pattern of COF-43 showed diffraction peaks with *d* spacings of 37.71, 21.99, 18.89, 14.37, 10.93, 8.72, and 7.22 Å and a small broad peak at ~3.6 Å. Analogous to COF-42, these values are in agreement with the 100, 110, 200, 210, 220, 320, 330, and 001 reflections of the hexagonal crystal structures **gra** and **bnn**. The unit cell was refined on a primitive hexagonal unit cell, affording parameters a = 43.164(12) Å and c = 3.590(17) Å (residuals: R_p = 1.68%, R_{wp} = 2.39%). Attempts to reconstruct electron density maps, perform simulated annealing, and complete the Rietveld refinements were prohibited by the data resolution of 3 Å. Furthermore, it is noteworthy that at this resolution, unique assignment of the framework topology as either **bnn** or **gra** was not possible for either COF. However, the great difference between the pore sizes for the two topologies facilitated this assignment using adsorption data, as discussed below.

Confirmation that the COF pores were activated was given by thermogravimetric analysis (TGA), which showed no weight loss for either COF until decomposition at 280 °C. The architectural stability and porosity of each COF was assessed by measuring gas adsorption isotherms on the fully activated samples. The Ar adsorption isotherm of COF-42 measured at 87 K (Figure 3a) showed a sharp uptake below P/P_0 = 0.05 with a step between P/P_0 = 0.05−0.20. This profile is best described as a type-IV isotherm, which is characteristic of mesoporous materials. The Brunauer−Emmett−Teller (BET) model was applied over the 0.12 < P/P_0 < 0.17 range of the isotherm, yielding a BET surface area of 710 m^2 g^{-1}. The 87 K Ar adsorption isotherm of COF-43 (Figure 3c) also possesses a type-IV shape, indicating that it is a mesoporous material. The application of the BET model over 0.15 < P/P_0 < 0.30 range afforded a surface area of 620 m^2 g^{-1}. Notably, the surface areas obtained for COF-42 and COF-43 are comparable to those of other 2D COFs with hexagonal pore systems.[2,4−8] A nonlocal density functional theory (NLDFT) model was fitted to the isotherms of COF-42 and COF-43 to estimate their pore size distributions and total pore volumes. The average pore sizes of 23 and 38 Å for COF-42 and COF-43, respectively (Figure 3b,d), are in good agreement with the expected pore sizes observed in the crystal simulations based on the **bnn** topology. The total pore volumes of COF-42 and COF-43 were also estimated to be V_p = 0.31 and 0.36 cm^3 g^{-1}, respectively.

We found that nonsubstituted terephthalohydrazides did not yield permanently porous materials.[35] It is presumed that the poor solubility of these in organic solvents leads to blockage of the pore network by unreacted starting material. The increased solubility of this component facilitated activation and resulted in the isolation of crystalline and permanently porous structures.

In conclusion, we have synthesized two new 2D porous COFs constructed from the dynamically reversible condensation of hydrazones. The molecular architectures of these robust COFs are constructed from functional groups that introduce novel polar and hydrogen-bonding units into the pore space, facilitating the exploration of enhanced properties.

■ ASSOCIATED CONTENT

Supporting Information. Detailed experimental procedures, including syntheses of COF-42 and COF-43; PXRD patterns, modeling techniques, and crystallographic data; FT-IR and CP-MAS NMR spectra; TGA traces; and gas adsorption data. This material is available free of charge via the Internet at http://pubs.acs.org.

■ AUTHOR INFORMATION

Corresponding Author
yaghi@chem.ucla.edu

Present Addresses
[§]Cornell University.
[∥]The University of Adelaide, Australia.
[⊥]The University of Tokyo, Japan.

■ ACKNOWLEDGMENT

Funding was provided by the DOE (DE-FG36-08GO18141). We thank Ms. C. Vogelsberg for helpful discussions. K.O. thanks the Japan Society for the Promotion of Science for financial support. O.M.Y. was supported by the WCU Program of KAIST.

■ REFERENCES

(1) Yaghi, O. M.; O'Keeffe, M.; Ockwig, N. W.; Chae, H. K.; Eddaoudi, M.; Kim, J. *Nature* **2003**, *423*, 705–714.
(2) Côté, A. P.; Benin, A. I.; Ockwig, N. W.; Matzger, A. J.; O'Keeffe, M.; Yaghi, O. M. *Science* **2005**, *310*, 1166–1170.
(3) El-Kaderi, H. M.; Hunt, J. R.; Mendoza-Cortés, J. L.; Côté, A. P.; Taylor, R. E.; O'Keeffe, M.; Yaghi, O. M. *Science* **2007**, *316*, 268–272.
(4) Côté, A. P.; El-Kaderi, H. M.; Furukawa, H.; Hunt, J. R.; Yaghi, O. M. *J. Am. Chem. Soc.* **2007**, *129*, 12914–12915.

(5) Tilford, R. W.; Gemmil, W. R.; zur Loye, H.-C.; Lavigne, J. J. *Chem. Mater.* **2006**, *18*, 5296–5301.
(6) Wan, S.; Guo, J.; Kim, J.; Ihee, H.; Jian, D. *Angew. Chem., Int. Ed.* **2008**, *47*, 8826–8830.
(7) Tilford, R. W.; Mugavero, S. J., III; Pellechia, P. J.; Lavigne, J. J. *Adv. Mater.* **2008**, *20*, 2741–2746.
(8) Wan, S.; Guo, J.; Kim, J.; Ihee, H.; Jiang, D. L. *Angew. Chem., Int. Ed.* **2009**, *48*, 5439–5442.
(9) Spitler, E. L.; Dichtel, W. R. *Nat. Chem.* **2010**, *2*, 672–677.
(10) Dogru, M.; Sonnauer, A.; Gavryushin, A.; Knochel, P.; Bein, T. *Chem. Commun.* **2011**, *47*, 1707–1709.
(11) Ding, X.; Guo, J.; Feng, X.; Honsho, Y.; Guo, J.; Seki, S.; Maitarad, P.; Saeki, A.; Nagase, S.; Jiang, D. *Angew. Chem., Int. Ed.* **2011**, *50*, 1289–1293.
(12) Wan, S.; Gándara, F.; Asano, A.; Furukawa, H.; Saeki, A.; Dey, S. K.; Liao, L.; Ambrogio, M. W.; Botros, Y. Y.; Duan, X.; Seki, S.; Stoddart, J. F.; Yaghi, O. M. Submitted.
(13) Hunt, J. R.; Doonan, C. J.; LeVangie, J. D.; Côté, A. P.; Yaghi, O. M. *J. Am. Chem. Soc.* **2008**, *130*, 11872–11873.
(14) Uribe-Romo, F. J.; Hunt, J. R.; Furukawa, H.; Klöck, C.; O'Keeffe, M.; Yaghi, O. M. *J. Am. Chem. Soc.* **2009**, *131*, 4570–4571.
(15) Kuhn, P.; Antonietti, M.; Thomas, A. *Angew. Chem., Int. Ed.* **2008**, *47*, 3450–3453.
(16) Furukawa, H.; Yaghi, O. M. *J. Am. Chem. Soc.* **2009**, *131*, 8875–8883.
(17) Doonan, C. J.; Tranchemontagne, D. J.; Glover, T. G.; Hunt, J. R.; Yaghi, O. M. *Nat. Chem.* **2010**, *2*, 235–238.
(18) Mendoza-Cortés, J. L.; Han, S. S.; Furukawa, H.; Yaghi, O. M.; Goddard, W. A., III. *J. Phys. Chem. A* **2010**, *114*, 10824–10833.
(19) Xiang, Z. H.; Cao, D. P.; Lan, J. H.; Wang, W. C.; Broom, D. P. *Energy Environ. Sci.* **2010**, *10*, 1469–1487.
(20) Assfour, B.; Seifert, G. *Microporous Mesoporous Mater.* **2010**, *133*, 59–65.
(21) Assfour, B.; Seifert, G. *Chem. Phys. Lett.* **2010**, *489*, 86–91.
(22) Han, S. S.; Furukawa, H.; Yaghi, O. M.; Goddard, W. A., III. *J. Am. Chem. Soc.* **2008**, *130*, 11580–11581.
(23) Garberoglio, G. *Langmuir* **2007**, *23*, 12154–12158.
(24) Rowan, S. J.; Cantrill, S. J.; Cousins, G. R. L.; Sanders, J. K. M.; Stoddart, J. F. *Angew. Chem., Int. Ed.* **2002**, *41*, 898–952.
(25) Skene, W. G.; Lehn, J.-M. P. *Proc. Natl. Acad. Sci. U.S.A.* **2004**, *101*, 8270–8275.
(26) See the Supporting Information.
(27) Elemental analysis. COF-42: Calcd (%): C, 61.46; H, 5.12; N, 15.81. Found (%): C, 54.45; H, 3.35; N, 14.50. COF-43: Calcd (%): C, 71.12; H, 5.17; N, 11.06. Found (%): C, 67.24; H, 5.31; N, 10.85.
(28) Emam, S. M.; El-Saied, F. A.; El-Enein, S. A.; El-Shater, H. A. *Spectrochim. Acta, Part A* **2009**, *72*, 291–297.
(29) Mangalam, N. A.; Panicker, C. Y.; Sheeja, S. R.; Kurup, M. R. P.; Mary, Y. S.; Raju, K.; Varghese, H. T.; Nair, V. M. *Int. J. Ind. Chem.* **2010**, *1*, 17–28.
(30) Alemany, L. B.; Grant, D. M.; Pugmire, R. J.; Alger, T. D.; Zilm, K. W. *J. Am. Chem. Soc.* **1983**, *105*, 2133–2141.
(31) Aldoshin, S. M.; Chuev, I. I.; Atovmyan, L. O.; Nedzvetskii, V. S.; Kulikov, A. S. *Russ. Chem. Bull.* **1991**, *40*, 74–76.
(32) O'Keeffe, M.; Peskov, M. A.; Ramsen, S. J.; Yaghi, O. M. *Acc. Chem. Res.* **2008**, *41*, 1782–1789.
(33) *Materials Studio*, version 5.0.0.0; Accelrys Software Inc.: San Diego, CA, 2009.
(34) See note 10 in ref 4.
(35) Uribe-Romo, F. J. Ph.D. Dissertation, University of California, Los Angeles, 2011.